

flush mounted at 3-m intervals along the outlet pipe. The signal from each transducer went through an emitter follower ($\sim 0.1\text{-}\mu\text{sec}$ rise time) to two scopes with appropriate sweep speeds and sensitivities that were determined from preshot estimates. The pressure transducers serve the dual purpose of providing TOA values and pressure-time histories for comparison with the calculations. Transducers 1, 3, and 5 were monitored with time-interval meters (TIM) to obtain microsecond accuracy on shock TOA with respect to the detonation signal.

III. NUMERICAL CODES AND INITIAL CONDITIONS

The two numerical codes HEMP⁹ and PUFL¹⁰ used in the present study are described in the literature. Both codes use finite-difference calculational techniques to advance, with respect to time, the partial differential conservation equations of continuum mechanics. The following paragraphs briefly discuss the use of these codes in numerically simulating the present experiment.

A. HEMP

HEMP is a two-dimensional Lagrangian code which is used here in cylindrical geometry. HEMP was used to simulate HE burn, the initiation of the air shock, and the radial wall motion in the HE region. The equations of state used in these calculations are given in Refs. 9 and 11.

B. PUFL

PUFL is used here to simulate the one-dimensional axially symmetric flow in the pipe. PUFL considers friction and heat transfer which are not considered in HEMP.

C. Numerical Calculation Model

Slight modifications of the actual experiment configuration (Fig. 1) were necessary in the numerical

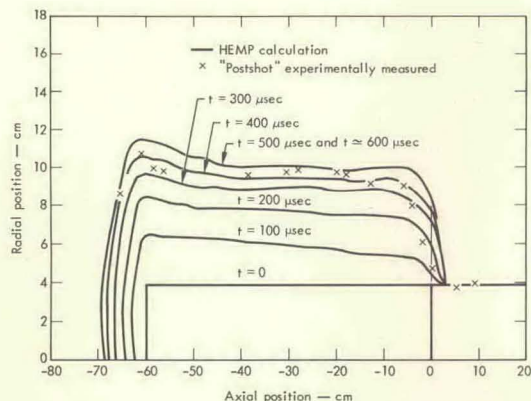


FIG. 3. Position of He-steel-wall boundary from HEMP plotted at 100- μsec intervals. "Postshot" measured values are also shown.

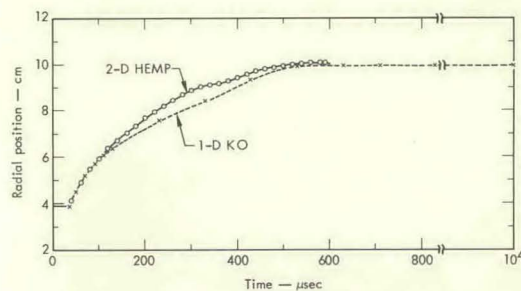


FIG. 4. Radial position of He-steel-wall boundary vs time (1-D KO code results and 2-D HEMP code results taken from axial midpoint of HE).

model illustrated in Fig. 2. These modifications are discussed below. Figure 2 also gives the yield strengths, dimensions, horizontal (L lines) and vertical (K lines) zoning, and other parameters pertinent to the calculations.

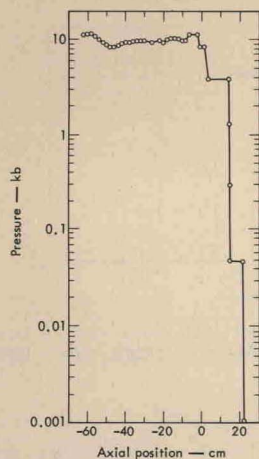
The calculations start with the initiation of detonation of the HE at the breach end of the 60-cm length of HE. No attempt was made to simulate the detonator or the plane-wave lens. Since the detonator and the plane-wave lens represent only a small portion (4.4 cm) of the total HE (64.4 cm), their omission is a minor perturbation. The end plates (Fig. 1) were also omitted in the numerical model. Other considerations in Fig. 2 are believed to be self-explanatory.

IV. THEORETICAL AND EXPERIMENTAL RESULTS

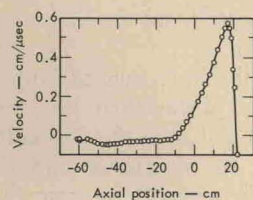
A. Source Region

For PBX 9404, with a detonation velocity of 0.88 cm/ μsec , the HEMP code indicates peak pressures behind the detonation front of $\sim 350\text{kbar}$.¹¹ The wall motion in the HE section is illustrated in Fig. 3, which shows the radial position of the inner cylindrical steel pipe that surrounds the HE, at 100- μsec intervals. At approximately 500 μsec , the radial expansion reaches its maximum. The pipe then undergoes a small radial contraction due to the elastic properties of the outer steel cylinder. To obtain the radial pipe expansion of this region after 600 μsec , a one-dimensional KO code⁹ calculation in cylindrical geometry was considered. The results of this calculation are given in Fig. 4 along with the first 600- μsec results from HEMP for comparison. Figure 4 shows the HEMP results plotted for the midpoint position of the HE where the end effects are reduced. Figure 4 implies that the radial motion essentially ceases after 600 μsec .

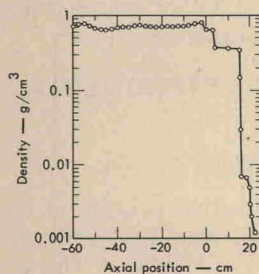
Axial and radial measurements of this HE region were taken postshot and are given in Fig. 3 for comparison with the calculated values. Radial variations at a given axial position were generally small (≤ 0.2 cm). Postshot observation also indicated that the inner steel cylinder remained intact with no fragmentation.



(a)



(b)



(c)

FIG. 5. HEMP code results at 100 μ sec for (a) pressure, (b) velocity, and (c) density.

Cracks in the axial direction occurred near the HE-air interface, which is consistent with late time (>1.0 msec) venting which was experimentally observed and is discussed below. Postshot measurements of the outer steel cylinder indicated that no permanent deformation occurred.

Framing camera coverage (90- μ sec interframe time) of the front section of the HE housing gave photographic evidence that HE gases vented from the source region. Venting to the atmosphere was first observed at 1.04 msec and continued until approximately 4.4 msec, after the HE was detonated. No gross motion of the outlet pipe or lead was noted for the 10-msec duration of the framing camera coverage. Postshot examination of the source region and framing film indicated that the venting path was radial through cracks in the inner steel pipe and lead housing. The

venting path was then axial through the shock-induced separation between the lead housing and outer steel cylinder. Consequently, the loss of HE gases from the driver section began much earlier than the 1.04 msec observed by photographic coverage of the front surface of the HE housing. This loss of driver gas was considered in the calculations presented later. It is shown that the loss of driver gas had a negligible effect on the TOA results, but it did affect the pressures well behind the shock front. Framing camera coverage of the rear section of the HE housing indicated that no venting occurred from this region for the duration (~ 10 msec) of the experiment.

At 100 μ sec, detonation of the HE is completed, and the air shock is starting to form. The velocity, density, and pressure from HEMP at 100 μ sec are shown in Figs. 5(a)-(c). These HEMP conditions are used as initial conditions for PUFL. Also, the pipe radius as a function of time and axial position from HEMP (Fig. 3) was used for the pipe-radius boundary condition in PUFL. Because of the KO results in Fig. 4, at times greater than 600 μ sec, the radii are assumed to remain constant.

The feasibility of using the quasi-one-dimensional PUFL code to simulate the pipe flow is illustrated in Fig. 6. This figure shows the pressure vs axial position as calculated by both HEMP and PUFL at 500 μ sec. Comparisons at earlier times give even closer agreement.

B. TOA Results

To correlate the optical and electronics measurements, a common time reference was provided by the electrical signal which initiated detonation of the plane-wave lens. The elapse time between the detonation signal and luminosity record for initiation of the air shock was experimentally measured as 80.6 μ sec. This luminosity record was obtained with the streaking camera and the aluminum-reflector-adapted light pipe mentioned previously. The elapse time compares with a 77.1- μ sec calculated elapse time which is obtained by

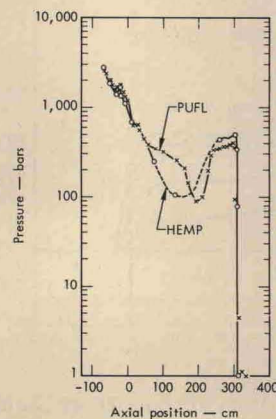


FIG. 6. Pressure vs axial position from both HEMP and PUFL codes at 500 μ sec.